Available online at www.sciencedirect.com
ScienceDirect
Ceramics International 37 (2011) 3071–3076
CERAMICS INTERNATIONAL
www.elsevier.com/locate/ceramint

Porous Si_3N_4 ceramics prepared via slip casting of Si and reaction bonded silicon nitride

Dongxu Yao [a,b], Yongfeng Xia [a], Yu-Ping Zeng [a,*], Kai-hui Zuo [a], Dongliang Jiang [a]

[a] State Key Laboratory of High Performance Ceramics and Superfine Microstructure, Shanghai Institute of Ceramics, Chinese Academy of Sciences, Shanghai 200050, China
[b] Graduate School of Chinese Academy of Sciences, Beijing 100039, China

Received 30 March 2011; received in revised form 6 May 2011; accepted 7 May 2011
Available online 13 May 2011

Abstract

Slip casting process combined with reaction bonded silicon nitride (RBSN) was used to prepare porous Si_3N_4 ceramic with near-net and complex shape. A butyl stearate (BS) coated process was introduced to restrain the hydrolysis of Si, and ammonium polyacrylate (NH_4PAA) was used to enhance the dispersion of coated Si. The measured oxygen content showed that the hydrolysis of Si was strongly prohibited by BS coating, and relatively low viscosity was obtained with the addition of 0.25–1.5 wt% NH_4PAA to the 60 wt% solid load slurry. 40–60 wt% solid load slurries were used for slip casting in the experiment. After vacuum degassing, slip casting, debindering and nitridation, a density of 1.57–1.92 g/cm^3 (porosity 50.9–40%) and a flexural strength of 47–108 MPa were obtained. The samples without vacuum degassing showed a large number of nanowires grown in the large pores.

Keywords: A. Slip casting; B. Porosity; D. Si_3N_4; RBSN

1. Introduction

Porous silicon nitride (Si_3N_4) ceramics has attracted significant attention for a number of industrial applications such as catalyst carriers, molten metal filters, and lightweight structural parts for elevated temperature applications [1–3]. Compared with sintered Si_3N_4 (SSN), reaction bonded Si_3N_4 (RBSN) showed advantages for its low cost of Si and the near-net shape capability [4]. Moreover, due to the small pore size, extensive internal oxidation can be avoided [5] and the flexural strengths appeared slightly improved at 1200–1400 °C in air [6].

The formation of Si powder compacts can be accomplished by a number of methods, including die pressing, isostatic pressing, slip casting [7–10], or gel casting [11,12]. Die pressing and isostatic pressing are usually used to fabricate simple shaped green body. Slip casting can be used to form a duplicate of the porous mould with complex shape. The consolidation of the slurries inside the mould takes place through the removal of the liquid phase of the slurries by capillary forces of the porous mould which absorbs the dispersing media to leave a shaped solid green body.

The characterizations of Si aqueous slurries have been reported by several authors [9,13–15]. Similar to SiC and Si_3N_4, the native SiO_2 on Si surface has a tendency to hydrolyze in water to form acidic silanol (Si–OH) surface groups. It would promote particle dispersion through the development of an electrical double-layer. However, the reaction between Si and H_2O was much serious as the following reaction (1), explosive evolution of gas can be observed.

$$Si + 2H_2O \rightarrow SiO_2 + 2H_2 \quad (1)$$

The newly formed SiO_2 acted as a protective layer against further reaction that is relatively stable under acidic or neutral pH conditions. But under alkaline conditions above pH value of 10, the passive SiO_2 layer can be destroyed according to reaction (2), and expose more new Si surface for reaction with H_2O as reaction (1).

$$SiO_2 + 2OH^- \rightarrow SiO_3^{2-} + H_2O \quad (2)$$

* Corresponding author. Tel.: +86 21 52415203; fax: +86 21 52415203.
E-mail address: yuping-zeng@mail.sic.ac.cn (Y.-P. Zeng).

0272-8842/$36.00
doi:10.1016/j.ceramint.2011.05.035

Hence, the condition of Si slip preparation was proposed to operate in acidic or weakly alkaline solution [10]. Ezis [16] indicated that stable slurry can be obtained after aging for 6 days when pH values were constant. However, the formation of thick SiO_2 layer would hinder the reaction between Si and N_2, and may lead to a low extent of nitridation. Glycerol trioleate (GTO) coated Si/BN powder was prepared and introduced by Liu et al. [17], and RBSN combined with slip-casting was used to fabricate porous Si_3N_4/BN ceramic composites.

In this paper, a butyl stearate (BS) coated process was introduced to restrain the hydrolysis of Si. The zeta potential, oxygen content and rheological properties of Si slips were measured, and the mechanical properties of the nitrided specimens were also characterized.

2. Experimental procedure

2.1. Materials

Commercially available Si powder (purity ≥99.9 wt%; d_{50} = 1.8 μm; 1.22 wt% oxygen; Peixian Tiannayuan Silicon Materials Co., Ltd., Xuzhou, Jiangsu province, China), butyl stearate (BS, SCRC, Shanghai, China), and ammonium polyacrylate (NH_4PAA, Lopon 885, BK Guilini, Siegburg, Germany) were selected as starting powder, coating agent and dispersant respectively. For the preparation of 4 wt% BS coated Si, 4 g of BS was firstly dissolved in anhydrous alcohol, then ball milled with 96 g Si and Si_3N_4 balls as media for 24 h in a plastic bottle. Finally, the mixture was dried at 60 °C to obtain 4 wt% BS coated Si powder.

2.2. Slip casting and nitriding program

4 wt% BS coated Si was firstly prepared, the slurries with different solid content were prepared by dispersing them in deionised water. The dispersant content was 1 wt% based on the weight of Si. The slurries were ball milled for 48 h and vacuum degassed to remove air bubble, then casted into plaster moulds with different shapes to obtain green bodies. The binder was removed from the green body by heating in vacuum to 900 °C at a heating rate of 2 °C/min. Compacts were then nitrided in the temperature range of 1100–1450 °C at heating rate of 10 °C/h in flowing N_2 atmosphere.

2.3. Characterization

The zeta potential was determined with a Zetaplus Analyzer (Zetaplus, Brookhaven Instruments, Holtsville, NY) by measuring the electrophoretic mobility of the particles using 0.001 M KCl as the electrolyte. The suspensions were ultrasonicated for 10 min before measurement. The pH values of the suspensions was adjusted manually by the addition of 0.25 M NaOH and 0.25 M HCl. Rheological behavior evaluation of the prepared slurry was carried out using a rotary viscometer (Rheometric Scientific SR5; Rheometric Scientific, Piscataway, NJ). Samples that had the binder removed were used for the oxygen content measurement. The oxygen content was measured with a Nitrogen/Oxygen Determinator TC600 (LECO Corporation, Michigan, USA).

Nitrided specimens were machined into a rectangle bar with a dimension of 3.0 × 4.0 × 36.0 mm to measure the flexural strength via the three point bending test (Instron 5566; Instron Company, Norwood, USA), the support distance of 30.0 mm and a cross-head speed of 0.5 mm/min were used. Four specimens were used to the get the average result. The bulk densities were determined by the Archimedes method using distilled water as medium. The phase compositions were determined by X-ray diffractometry (XRD; D/MAX-RBX, Rigaku, Osaka, Japan) with CuKa radiation. Scanning electronic microscopy (SEM; JEOL, JSM-6390, Japan) was used to observe the morphologies of the fracture surfaces.

3. Results and discussion

3.1. Zeta potential measurement

Zeta potentials of raw Si, 2 wt% BS coated Si, and 4 wt% BS coated Si suspensions with 1 wt% (dry weight basis) and without NH_4PAA addition as a function of pH value are shown in Fig. 1. It can be seen that iso-electrical point (IEP) of raw Si is about pH = 2.8. Si powder exposure to water leads to surface hydroxylation, enabling acid or base reactions to take place as

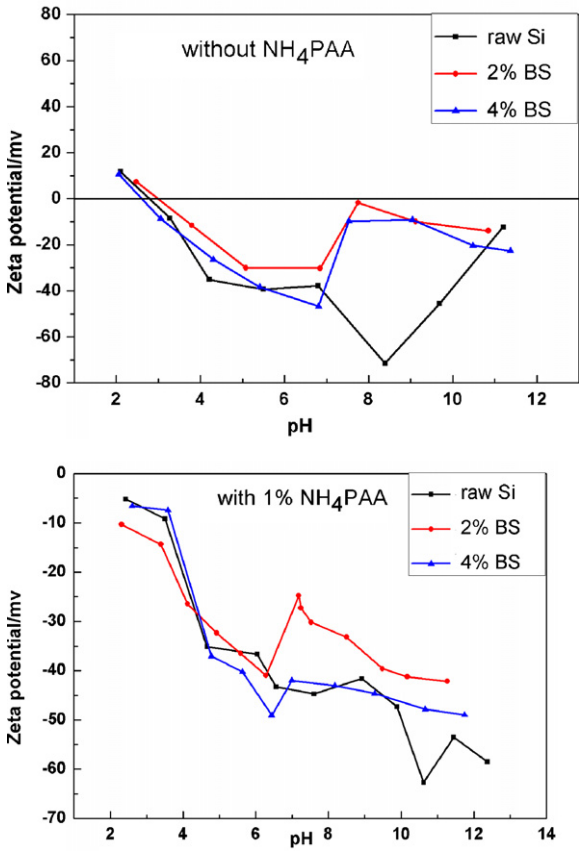

Fig. 1. Zeta potentials of raw Si, 2 wt% BS coated Si, and 4 wt% BS coated Si suspensions with 1 wt% (dry weight basis) and without NH_4PAA addition as a function of pH.

shown by reactions (3) and (4),

$$Si{-}OH + H_2O^+ \rightarrow SiOH_2^+ + H_2O \quad (3)$$

$$Si{-}OH + OH^- \rightarrow SiO^- + H_2O \quad (4)$$

The net surface charge is positive at pH values below IEP and change to negative at pH values beyond IEP. The zeta potential of Si powder is similar to that of the previous report by Rao et al. [9], which indicated that the optimum pH values of Si dispersion were 4 and 8. The decrease of zeta potential at higher pH values of 9–11 is attributed to the higher ionic strength of the base electrolyte, resulting in the compression of electrical double layer [18].

In Fig. 1(a), raw Si, 2 wt% BS coated Si, and 4 wt% BS coated Si showed a similar zeta potential at the pH range of 2–6.8, but the coated samples showed low absolute zeta potential value compared with raw Si at the pH range of 7.4–11. As zeta potential arises out of net effective surface charge on the particles in the suspension, it directly reflects the dispensability of Si particles in a medium. At the pH range of 7.4–9, the low absolute zeta potential is difficult to obtain high solid load slurry with low viscosity. Although it seems to have a well dispersed slurry at the pH range of 5–6.8, actually it is hard to obtain fluid slurry for the 60 wt% solid load sample with coated Si in this experiment. With the addition of 1 wt% NH_4PAA, the absolute zeta potential was increased at pH >6. The well-dispersed slurry can be obtained at the pH range of 6–8.

3.2. The effect of NH_4PAA on oxygen content and rheological properties of Si slurry

Some authors [10] evaluated the hydrolysis of Si powder by measuring the amount of H_2. In this study, the oxygen content was measured to evaluate the hydrolysis of Si, as shown in Fig. 2. At first, the oxygen content was measured on 40 wt% solid content slurries coated with varied SB contents, NH_4PAA was not added in this stage. The oxygen content of raw Si was 1.22 wt%. When the slurry was ball milled for 48 h without coating treatment, the oxygen content increased into 2.96 wt%.

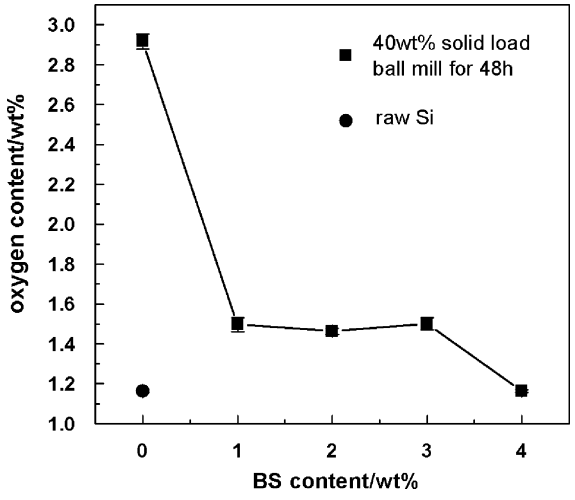

Fig. 2. Oxygen content of Si powder at various BS coated contents.

As Si was coated with SB content of 1–3 wt%, the oxygen content was limited at around 1.6 wt%. The oxygen content of Si powder coated with 4 wt% SB was 1.24 wt%, which was almost the same as that of the raw Si. This means that the 4 wt% SB coated Si was effective against hydrolyzation.

The 60 wt% solid load Si slurry with 4 wt% SB coating can hardly form a fluid phase without dispersant. With NH_4PAA addition ranging from 0.25 to 1.5 wt%, a fluid slurry was obtained. The viscosity of the slurry versus shear rate is shown in Fig. 3(a). The slurries exhibit shear-thinning character, which is useful to operate in slip casting. Further addition of dispersant has no beneficial effect on the dispersion of the slurry. The addition of dispersant caused a slight increase in oxygen content. The highest oxygen content was 1.63 wt% with 0.5 wt% NH_4PAA; however, the viscosity was 0.21 Pa S^{-1} at shear rate of 100 s^{-1}. The viscosity at shear rate of 100 s^{-1} seems to have an opposite trend with the oxygen content, as shown in Fig. 3(b). Based on the above result, a stable, hydrophobic slurry for slip casting could be obtained by the following steps: (a) coating Si particles with 4 wt% BS; (b) using 0.25–1.5 wt% NH_4PAA to improve the dispensability of

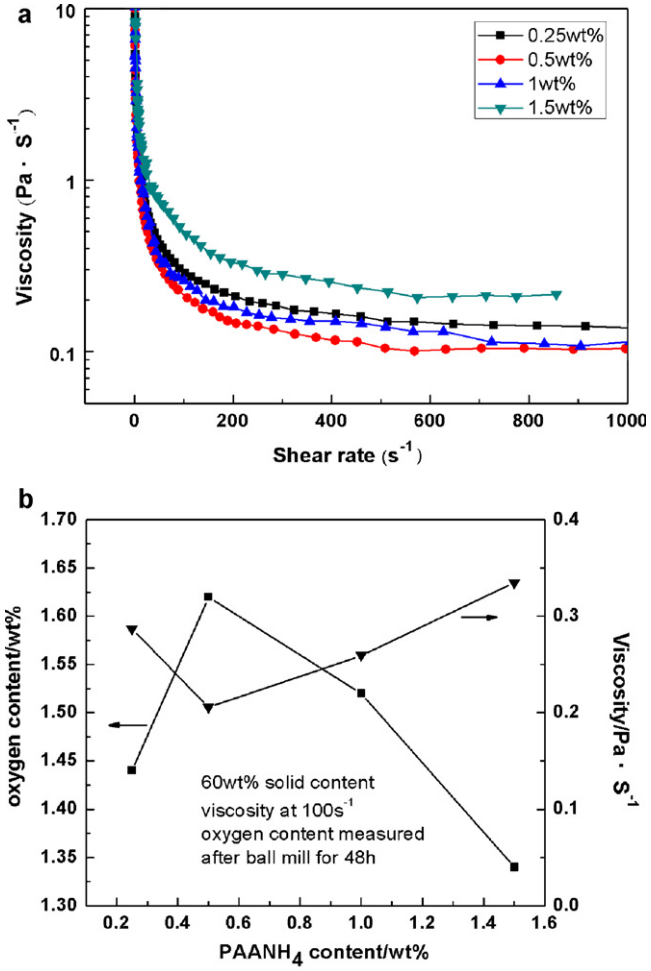

Fig. 3. (a) The shear rate–viscosity curve of 60 wt% solid content slurry with 4 wt% SB coated Si at different NH_4PAA contents; (b) the oxygen content and viscosity at shear rate of 100 s^{-1} at different NH_4PAA contents.

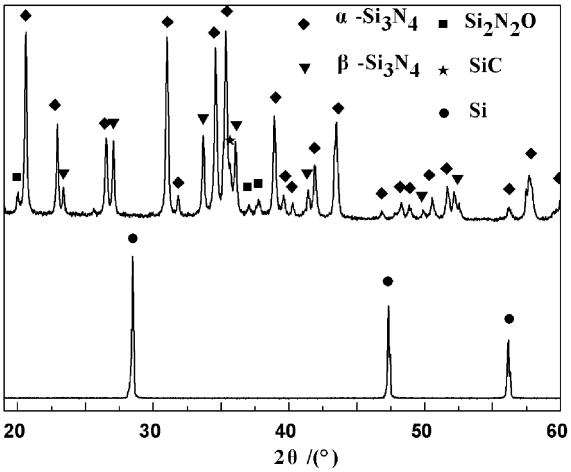

Fig. 4. X-ray diffraction pattern of the raw Si and nitrided specimens.

Fig. 5. Photo of green crucible bodies prepared by 40 wt% solid load slurries.

the slurry; (c) controlling the pH of the suspension between 6 and 8.

3.3. Slip casting of Si slurry and the properties of RBSN

Fig. 4 shows XRD results of the raw Si and the sample after nitridation. After nitridation, the main phases consist of α-Si_3N_4, β-Si_3N_4, the peaks of residual Si are too weak to identify. Small peaks of SiC and Si_2N_2O also appear in the XRD pattern. Fig. 5 shows the green crucible bodies prepared by 40 wt% solid load slurries. The inner surfaces were very smooth without any apparent defects. A homogeneous packing of the particles can be observed by the scanning electron micrograph shown in Fig. 6(a).

The formation of Si_3N_4 nanowires or whiskers in RBSN was reported by several authors [19–23]. According to their studies, vapor–liquid–solid (VLS) and vapor–solid (VS) mechanisms are the main explanations for the growth of Si_3N_4 nanowires. The impurities in Si powder, such as Fe, can form a eutectic $FeSi_2$ which was lower than the Si melting point as much as 200 °C [19]. So the formation of liquid phase combined with Fe impurity in the beads supported the VLS mechanism [20]. In the VS mechanism, the key is the formation of SiO gas phase as

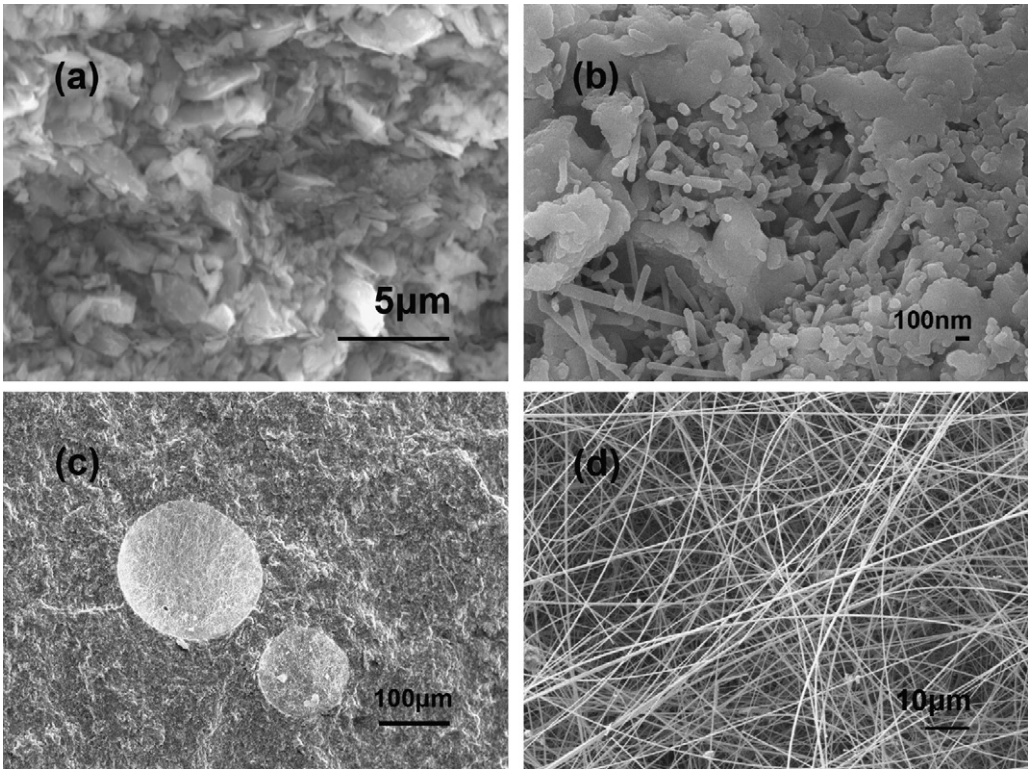

Fig. 6. Scanning electronic microscope (SEM) of the specimens. (a) The fracture surface of the green body; (b) the fracture surface of the nitrided specimen; (c) the fracture surface of the nitrided specimen with large pore; (d) nanowires grew in the large pore of the nitrided specimen.

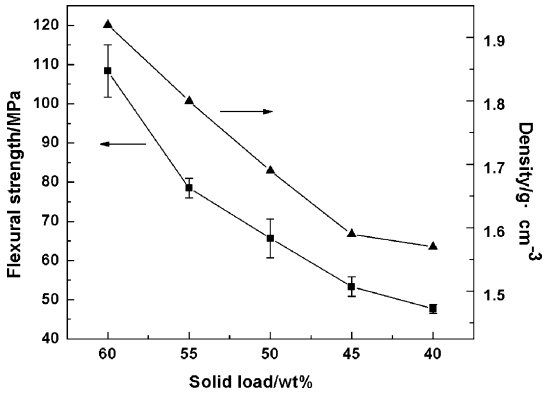

Fig. 7. The flexural strength–density curve as a function of solid load.

reaction (5) [21] and (6) [22], and the formation of Si_3N_4 nanowires as reactions (7) and (8) [22]:

$$SiO_2(s) + H_2(g) \rightarrow SiO(g) + H_2O(g) \quad (5)$$

$$SiO_2(s) + C(s) \rightarrow SiO(g) + CO(g) \quad (6)$$

$$3SiO(g) + 3C(s) + 2N_2(g) \rightarrow Si_3N_4(s) + 3CO(g) \quad (7)$$

$$3SiO(g) + 3CO(s) + 2N_2(g) \rightarrow Si_3N_4(s) + 3CO_2(g) \quad (8)$$

In this experiment, some residual carbon must exist after debindering, which may lead to the formation of SiO phase. The nanowire morphology was hard to determine in the nitrided samples with vacuum degassing process under low-magnification SEM. The fracture surface of the nitrided sample was typical morphology of RBSN, as shown in Fig. 6(b). The stacked Si particles transformed into a strong bonded matrix. Nanowires can be observed in the interparticle voids. But in the samples without vacuum degassing process, large pores around 100 μm were observed, as shown in Fig. 6(c). A main source of the large pores was air bubbles introduced during the preparation of the slurry, as shown in Fig. 6(d). The pores filled with a large quantity of nanowires, the large pore offers enough space for nanowires to grow which was in coincidence with the result by Hu et al. [23], who used benzoic acid balls (0.8 mm) as pore-forming agent. The nanowires in the large pores can hardly make up for this critical defect. Its flexural strength was inferior to the specimens without large pores.

In early research on the mechanism of nitridation, considerable attention was paid to the nitridation of high purity single phase Si with gettered N_2 to minimize the influence of impurity [24–27]. The observation of large pores between the Si–Si_3N_4 layers confirmed the hypothesis that the growth of Si_3N_4 was controlled by Si vapor transportation to the Si_3N_4 nuclei site. Although SiO is seen as an impurity gas phase in the nitriding process, it may also play a role in developing high flexural strength materials. At the early stages of nitriding process, the main reaction was elimination of the necks between Si particles, followed by the development of a continuous skeletal network of Si_3N_4 within the pore space of the original compact [28]. For SiO acted as the transport medium instead of Si vapor, the microstructure turned to be like a fine network rather than coarse Si_3N_4 surface. The higher the partial pressure of SiO, the finer the nitrided network and the better the development of a continuous skeletal network of Si_3N_4 [21]. This network contributed to the flexural strength of the final nitrided specimens. The various density and flexural strength of nitrided specimens as a function of the solid content are presented in Fig. 7. Densities of 1.57–1.92 g/cm^3 (porosities of 50.9–40%), flexural strengths of 47–108 MPa were obtained, the flexural strength decreased with decreasing density. As solid load was lower than 40 wt%, the nitrided density (1.57 g/cm^3) was similar to that of the 45 wt% solid load (1.59 g/cm^3). It is difficult to get much lower density compact due to the drive of capillary force during slip casting.

4. Conclusions

Slip casting process combined with reaction bonded silicon nitride (RBSN) was used to prepare porous Si_3N_4 ceramic in a low cost way with near-net and complex shape. The following conclusions were obtained:

(1) The results showed that the hydrolysis of Si was strongly prohibited by coated with 4 wt% BS as the oxygen content was reduced from 2.96 wt% to 1.24 wt%. Low viscosity was obtained with the addition of 0.25–1.5 wt% NH_4PAA to the 60 wt% solid load slurry.
(2) The main phases of the nitrided specimens consist of α-Si_3N_4, β-Si_3N_4. Small amounts of SiC and Si_2N_2O also appear in the XRD pattern, the peaks of residual Si are too weak to identify.
(3) The specimens without vacuum degassing process, large pores were left in the green body, during nitridation, a large quantity of nanowires were grown in the pores for providing growth space. In the specimens with vacuum degassing process, nanowires can be observed in the interparticle voids.
(4) By controlling the solid load content, nitrided densities of 1.57–1.92 g/cm^3 (porosities of 50.9–40%), and flexural strengths of 47–108 MPa were obtained, the flexural strength decreased with decreasing density.

Acknowledgement

This work was supported by National Natural Science Foundation of China (Nos. 50872142 and 50902140).

References

[1] R.W. Rice, Porosity of Ceramics, Marcel Dekker Inc., New York, 1998.
[2] J.F. Yang, G.J. Zhang, N. Kondo, T. Ohji, Synthesis and properties of porous Si_3N_4/SiC nanocomposites by carbothermal reaction between Si_3N_4 and carbon, Acta Mater. 50 (2002) 4831–4840.
[3] J.H. She, J.F. Yang, D.D. Jayaseelan, N. Kondo, T. Ohji, S. Kanzaki, et al., Thermal shock behavior of isotropic and anisotropic porous silicon nitride, J. Am. Ceram. Soc. 86 (2003) 738–740.
[4] A.J. Moulson, Reaction-bonded silicon nitride: its formation and properties, J. Mater. Sci. 14 (1979) 1017–1051.
[5] F. Porz, F. Thummler, Oxidation mechanism of porous silicon-nitride, J. Mater. Sci. 19 (1984) 1283–1295.

[6] F.L. Riley, Silicon nitride and related materials, J. Am. Ceram. Soc. 83 (2000) 245–265.
[7] R.M. Williams, A. Ezis, Slip casting of silcon shapes and their nitriding, Am. Ceram. Soc. Bull. 62 (1983) 619, 607-610&.
[8] M.D. Sacks, G. Scheiffele, Properties of silicon suspensions and slip-cast bodies, Am. Ceram. Soc. Bull. 63 (1984) 1476–11476.
[9] R.R. Rao, H.N. Roopa, T.S. Kannan, The characterisation of aqueous silicon slips, J. Eur. Ceram. Soc. 19 (1999) 2763–2771.
[10] R. Dillinger, J. Heinrich, J. Huber, Slip-cast hot isostatically pressed silicon nitride gas turbine components, Mater. Sci. Eng. A 109 (1989) 373–378.
[11] Q.G. Zhang, M.Y. Gu, Rheological properties and gelcasting of concentrated aqueous silicon suspension, Mater. Sci. Eng. A 399 (2005) 351–357.
[12] X.M. Pang, M.X. Xu, H. Liang, X.L. Li, H.M. Ji, Rheological properties and thixotropy model of concentrated aqueous silicon slurry for gel casting, Colloid Surf. A 317 (2008) 136–145.
[13] V.A. Hackley, U. Paik, B.H. Kim, S.G. Malghan, Aqueous processing of sintered reaction-bonded silicon nitride. 1. Dispersion properties of silicon powder, J. Am. Ceram. Soc. 80 (1997) 1781–1788.
[14] Q. Zhang, W. Li, M. Gu, Y. Jin, Dispersion and rheological properties of concentrated silicon aqueous suspension, Powder Technol. 161 (2006) 130–134.
[15] R.R. Rao, H.N. Roopa, T.S. Kannan, Dispersion, slip casting and reaction nitridation of silicon–silicon carbide mixtures, J. Eur. Ceram. Soc. 19 (1999) 2145–2153.
[16] A. Ezis, Fabrication and properties of slip-cast silicon nitride, Ceram. High Perform. Appl. (1974) 207–222.
[17] J.X. Liu, B. Yuan, G.J. Zhang, Y.M. Kan, P.L. Wang, Properties of porous Si_3N_4/BN composites fabricated by RBSN technique, Int. J. Appl. Ceram. Technol. 7 (2010) 536–545.
[18] M.D. Sacks, G.W. Scheiffele, Properties of silicon suspensions and slip-cast bodies, Ceram. Eng. Sci. Proc. 6 (1985) 1109–1123.
[19] P. Arundale, A.J. Moulson, Microstructural changes during argon-sintering of silicon powder compacts, J. Mater. Sci. 12 (1977) 2138–2140.
[20] D.R. Messier, P. Wong, Kinetics of nitridation of Si powder compacts, J. Am. Ceram. Soc. 56 (1973) 480–485.
[21] M.W. Lindley, D.P. Elias, B.F. Jones, K.C. Pitman, Influence of hydrogen in the nitriding gas on the strength, structure and composition of reaction-sintered silicon-nitride, J. Mater. Sci 14 (1979) 70–85.
[22] A.W. Weimer, G.A. Eisman, D.W. Susnitzky, D.R. Beaman, J.W. McCoy, Mechanism and kinetics of the carbothermal nitridation synthesis of alpha-silicon nitride, J. Am. Ceram. Soc. 80 (1997) 2853–2863.
[23] H.J. Hu, W.C. Zhou, F. Luo, D.M. Zhu, J. Xu, A new synthesis method for producing Si_3N_4 whiskers by heat treating porous Si objects, J. Am. Ceram. Soc. 91 (2008) 3800–3802.
[24] H.M. Jennings, B.J. Dalgleish, P.L. Pratt, Reactions between silicon and nitrogen. Part 2. Microstructure, J. Mater. Sci. 23 (1988) 2573–2783.
[25] B.J. Dalgleish, H.M. Jennings, P.L. Pratt, The formation of nitrides on pure silicon surfaces, Special Ceram. 7 (1981) 85–96.
[26] A. Atkinson, A.J. Moulson, E.W. Roberts, Nitridation of high-purity silicon, J. Am. Ceram. Soc. 59 (1976) 285–289.
[27] A. Atkinson, P.J. Leatt, A.J. Moulson, E.W. Roberts, A mechanism for the nitridation of silicon powder compacts, J. Mater. Sci. 9 (1974) 981–984.
[28] B.F. Jones, K.C. Pitman, M.W. Lindley, The development of strength in reaction sintered silicon nitride, J. Mater. Sci. 12 (1977) 563–576.